

Microcrystalline silicon and micromorph tandem solar cells

H. Keppner¹, J. Meier², P. Torres², D. Fischer², A. Shah²

¹University of Applied Science, 7 avenue de l'Hôtel-de-Ville, CH-2400 Le Locle, Switzerland (E-mail: keppner@eicn.ch)

²Institute of Microtechnology, University of Neuchâtel, A.-L. Breguet 2, CH-2000 Neuchâtel, Switzerland

Abstract. “Micromorph” tandem solar cells consisting of a microcrystalline silicon bottom cell and an amorphous silicon top cell are considered as one of the most promising new thin-film silicon solar-cell concepts. Their promise lies in the hope of simultaneously achieving high conversion efficiencies at relatively low manufacturing costs. The concept was introduced by IMT Neuchâtel, based on the VHF-GD (very high frequency glow discharge) deposition method. The key element of the micromorph cell is the hydrogenated microcrystalline silicon bottom cell that opens new perspectives for low-temperature thin-film crystalline silicon technology. According to our present physical understanding microcrystalline silicon can be considered to be much more complex and very different from an ideal isotropic semiconductor. So far, stabilized efficiencies of about 12% (10.7% independently confirmed) could be obtained with micromorph solar cells. The scope of this paper is to emphasize two aspects: the first one is the complexity and the variety of microcrystalline silicon. The second aspect is to point out that the deposition parameter space is very large and mainly unexploited. Nevertheless, the results obtained are very encouraging and confirm that the micromorph concept has the potential to come close to the required performance criteria concerning price and efficiency.

The justification of worldwide, intensified research on thin-film solar cells is not based on a lack of success in the efficiency performance of wafer-based silicon or GaAs technologies. It is based on a lack of hope in the cost reduction potential of wafer-based technology. Indeed, in order to render photovoltaics a competitive energy source in future, it is imperative to adopt the approach of low-cost solar cells. However, the abandoning of the “safe” wafer, with its phenomenally high diffusion lengths of hundreds of micrometers, has so far been, without any exceptions, always accompanied by a significant loss in efficiency. The efficiency drops down to less than a half, when compared to the record efficiencies of 24% achieved with wafers [1]. Nevertheless, the attraction of all thin-film concepts is based on the fact that the (generally expensive) semiconductor can here be deposited

directly on low-cost large-area substrates. Furthermore, in all thin-film concepts, the cell must not be self-supporting and its thickness can therefore be chosen based on the absorption requirements.

Thin-film solar cells based on compound semiconductors such as CdTe and Cu(In, Ga)Se₂ (CIGS), have attracted much attention in the past due to the remarkable work of many groups [2–4]; silicon-based thin-film solar cells were until recently exclusively limited to activities related to amorphous silicon (a-Si:H). Amorphous silicon technology has now achieved an industrial level [5, 6] and is economically competitive, contributing thereby to a reduction of the price per W_p. However, a-Si:H has always been associated with low efficiencies and with further efficiency losses during operation due to the Staebler–Wronski effect (SWE). Still, the low deposition temperature of around 200 °C and the application of the monolithic series connection technique for module manufacturing [6, 7] were generally considered as key features in order to obtain low manufacturing costs.

Polysilicon material deposited at high temperatures by the CVD process is basically limited by the difficulty in finding low-cost substrates that have, on one hand, the same thermal expansion coefficient as silicon, and on the other hand, do not contaminate the growing layer [8]. Furthermore, CVD or PECVD processes for the deposition of thin crystalline silicon layers will in general lead to layers with gap states and defects at the grain-boundary zones. These gap states act, as recombination centers, and, furthermore they screen the internal electrical field necessary for carrier collection within *p-i-n*-type solar cells [9]. In particular, for solar cell applications, the ratio of collection length to cell thickness (given by the absorption requirements) must be as large as possible. Note that due to the many grains and grain boundaries present in crystalline thin-films this ratio appears at first sight to be less advantageous for polysilicon than for amorphous silicon; hereby, the particularly strong absorption of a-Si:H overcompensates the poor electronic quality of this material.

Hydrogenated microcrystalline silicon ($\mu\text{c-Si:H}$) was originally introduced by Veprek et al. [10–12] and is nowadays generally obtained by a PECVD process using a mixture of silane and hydrogen. Due to its efficient doping properties, both for *n*-type as well as *p*-type material, $\mu\text{c-Si:H}$ was from the beginning successfully used as ohmic contact layers in so-

lar cells and in thin-film transistors. To use microcrystalline silicon alone as an active absorber layer in solar cells was, due to the reasons mentioned above, for many years not seriously taken into account for solar cell applications.

Recently, three different approaches have shown experimentally shown that microcrystalline silicon can indeed be, if suitably deposited, a very interesting active absorber material for photovoltaic solar cells:

1. The VHF-GD (very high frequency glow discharge) technique pioneered by IMT Neuchâtel [13] was the method which demonstrated for the first time the deposition of entirely microcrystalline cells in *p-i-n* and inverted *n-i-p* structures with reasonable efficiencies at 200 °C deposition temperature [14–21]. Using a *p-i-n* structure, AM1.5 efficiencies of 8.5% could recently be achieved [20, 21]. A review on the state of the art and the milestones of this VHF approach forms the objectives of this article.
2. A further successful approach on $\mu\text{c-Si:H}$ -based solar cells was achieved by the researchers of Kaneka Co. Ltd. [22]; this group uses a PECVD process at substrate temperatures of about 500–550 °C. Here, cell efficiencies of 10.1% were recently reported for a 2- μm -thick thin-film silicon cell.
3. The third approach for $\mu\text{c-Si:H}$ solar cell deposition is constituted by the catalytic CVD or “hot wire” technique. However, so far the success here was limited at least as far as results on solar cells are concerned [23–25].

Thus, the VHF-GD process plays a favorable role in the deposition of hydrogenated microcrystalline silicon at low substrate temperatures and this is presumably due to the following reasons:

1. At a given power dissipated into the plasma, the peak-to-peak voltage at the electrodes is strongly reduced under VHF conditions, as compared to 13.56 MHz. A lower peak-to-peak voltage is also an indication of a lower ion peak energy [26, 27]. In other words, the critical threshold energy for defect formation in the growing Si-layer due to bombardment by Si^+ ions or ionized silane radicals, is reduced by the use of VHF plasma conditions [28–30].
2. The higher electron density in the VHF plasma causes both enhanced silane dissociation and higher hydrogen dissociation; the latter gives rise to an increased atomic hydrogen exposure of the film surface and, by that, an intensified grain-boundary passivation.
3. The enhanced deposition rate due to the pronounced dissociation of silane allows a reduction of unwanted contaminants in the growing film [31–33].

In Sect. 1 of this article are material issues and deposition aspects of $\mu\text{c-Si:H}$ summarized. Sect. 2 describes the state of the art of $\mu\text{c-Si:H}$ single-junction solar cells. Section 3 gives the present state of research on micromorph tandem cells in comparison to other low-temperature-deposited crystalline silicon-based solar cells.

1 Microcrystalline silicon thin films

1.1 Midgap material (intrinsic layers with Fermi level E_F at midgap)

As-deposited intrinsic microcrystalline silicon tends in general to have a *n*-type character. This was already described

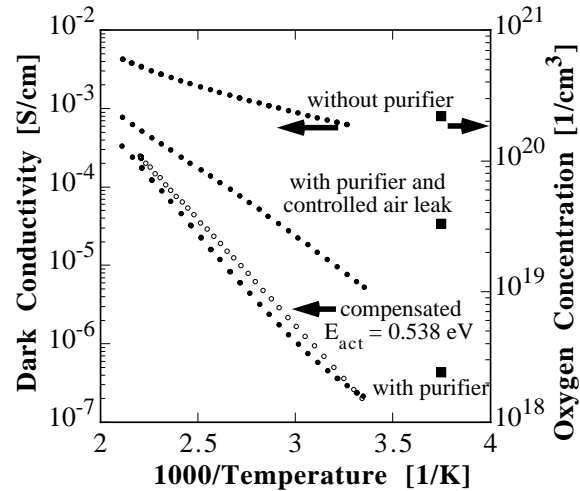


Fig. 1. Correlation between the activation energy of the dark conductivity and the oxygen concentration in $\mu\text{c-Si:H}$ thin films [15]

by Veprek et al. [34]. The origin of this *n*-type character was attributed either to the large amount of defects or to the large amount of oxygen incorporated in these films [34–37]. However, by the addition of small quantities of boron it was possible to compensate this *n*-type character, and, to push the Fermi level to midgap [14, 16, 17, 35, 37], achieving thus, efficiencies of 4.6% in a single-junction *p-i-n* solar cell [14]. This technique was called the “microdoping” technique; it was found to be technically extremely delicate, both in its reproducibility with respect to obtain the desired midgap character of the material. What is surprising, however, is the fact, that the *addition* of further impurities (boron) improves the efficiency of the solar cell. One therefore has to conclude that the midgap character of the base material is of primary importance rather than the concentration of (certain) impurities. In order to check the origin of the *n*-type character of as-grown $\mu\text{c-Si:H}$, in a further step the oxygen incorporation was reduced by using a gas purifier during deposition (purifying technique [15, 31–33]). Thereby, layers with midgap character could be obtained provided the oxygen contamination was low; this implies that the formation of defects that cause a *n*-type character in the growing $\mu\text{c-Si:H}$ layer is either nonexistent or very low (at least for $\mu\text{c-Si:H}$ grown by the VHF-GD).

Figure 1 summarizes these results [15]: The midgap character was monitored by measuring the activation energy E_{act} of the dark conductivity (for midgap material E_{act} should be half of the energy gap). The activation energy could be clearly linked to the concentration of active oxygen impurities and also to the efficiency of the solar cells (see also Fig. 6). Thus, it can be concluded that the midgap character is one of the key requirements for $\mu\text{c-Si:H}$ absorber layers with respect of carrier collection of *p-i-n* solar cell.

1.2 Optical properties

For solar cell applications, as mentioned before, the collection length (i.e. the carrier drift and/or diffusion lengths) must be larger than the thickness of the cell (the thickness of the cell, being in its turn, determined by the penetration depth of

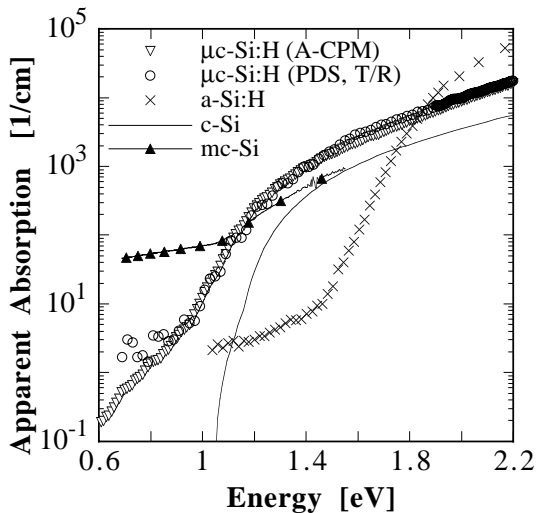


Fig. 2. Apparent absorption of $\mu\text{c-Si:H}$ in comparison with the absorption of a-Si:H, of monocrystalline Silicon (c-Si) and of multicrystalline silicon (mc-Si) [38]

light, particularly for photon energies close to the energy of the gap). The typical absorption spectrum of microcrystalline silicon in Fig. 2, as measured both by PDS (photothermal deflection spectroscopy) and by CPM (constant photocurrent method), shows clearly that the optical energy gap of $\mu\text{c-Si:H}$ is somewhere around 1 eV. This observation gives rise to the conclusion that the absorption of microcrystalline silicon is closer to that of wafer-based c-Si [38] or to that of silicon on sapphire (SOS) and very different from that of amorphous silicon (a-Si:H).

VHF-GD-deposited microcrystalline silicon clearly has an enhanced apparent absorption as compared to wafer-based silicon or epitaxially grown silicon on sapphire (SOS). An explanation for this effect was given by Vanecek et al. [39]: The enhanced apparent absorption of typical VHF-deposited $\mu\text{c-Si:H}$ layers is mainly due to the scattering of light at the as-grown “rough” surface of the layers. In a more recent work [40], this scattering effect could be artificially suppressed by a subsequent film polishing step; the reduced absorption of polished $\mu\text{c-Si:H}$ thereby obtained is comparable to that of SOS material; thus this experiment can be considered as the proof that the enhancement of the apparent absorption is indeed mainly due to surface roughness. Note, that this surface scattering effect is, in fact, crucial for thin-film solar cells because an increase in apparent absorption means that thinner *i*-layers can be used; this has three advantages. First, the deposition time of the absorber layer is reduced. Second, the material input is reduced. Third, a better ratio between the collection length and the cell thickness is established. In other words, a thinner absorber layer has a direct impact on both cell efficiency and on the fabrication costs. This fact lets hydrogenated microcrystalline silicon become *the bridge* between two technologies: between conventional crystalline silicon technology and amorphous silicon large-area thin-film technology.

1.3 Morphology

The preferential columnar growth along the [220] crystalline direction could be identified by X-ray diffraction and

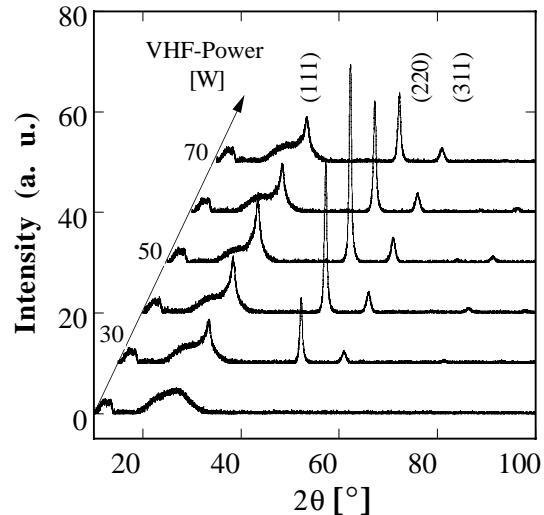


Fig. 3. X-ray diffraction pattern of layers deposited at a fixed dilution ratio of 7.5% of silane into hydrogen plus silane. At a low VHF power level of 20 W the morphology is amorphous, but at higher VHF power we can clearly see an onset of crystalline growth, according to [28]

SEM (scanning electron microscopy) investigations [28]. The morphology of the films in terms of crystalline orientation could be modified in a wide range, by varying of deposition parameters, as shown in Fig. 3 for example. In another series of deposition, at a dilution of 5% silane in hydrogen, the [111] diffraction peak was found to be completely suppressed [28].

We may conjecture that for solar cell applications the ideal case would be the total suppression of grain-boundaries parallel to the substrate. In such a case the detrimental effect of internal barriers and potential fluctuations [9] which give rise to enhanced bulk recombination and/or field losses could be avoided. Looking at such a desired columnar structure and the results so far obtained, one may suggest that VHF-GD is a suitable method permitting one to come close to this ideal case.

Figure 3 demonstrates, that in contrast to amorphous silicon, microcrystalline silicon ($\mu\text{c-Si:H}$) has a wide variety of possible structural appearances. There is not just a standard form of $\mu\text{c-Si:H}$, there is a large field of different forms of $\mu\text{c-Si:H}$ materials to be explored. Today we are just beginning to understand the nature of this semiconductor.

1.4 Deposition rate of microcrystalline silicon

In our initial statement it was argued that requirements of modern thin-film solar-cell concepts have to take into account economic aspects for device manufacturing rather than only high-efficiency objectives. Hence, already at the laboratory stage, a process with a high deposition rate is imperative. The importance of the deposition rate for $\mu\text{c-Si:H}$ is illustrated in Fig. 4. Note that a 2- μm -thick $\mu\text{c-Si:H}$ solar cell requires more than 5 h of deposition time if a conventional glow discharge process at 13.56 MHz is used (rate $< 1 \text{ \AA/s}$). This is definitely too long at the throughputs needed for solar cell manufacturing.

Different processes show promise that very high deposition rates for thin-film crystalline silicon can be achieved: hot wire experiments revealed deposition rates of crystalline

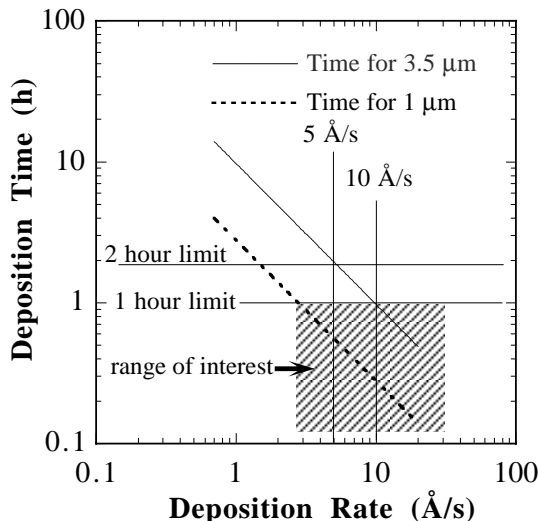


Fig. 4. Deposition time for $\mu\text{c-Si:H}$ films in function of the deposition rate. The dashed region represents the field of interest for photovoltaic applications [28]

thin-films as high as 37 \AA/s [24] under similar conditions as generally used for PECVD. Other approaches using arc discharges (plasma torches) also showed high deposition rates [41]. However, such highly confined plasma discharges are generally not directly transferable to large-area solar module manufacturing. Furthermore so far no solar cells with reasonable efficiencies (not even small areas) have been obtained at these high rates neither with hot-wire deposition nor with arc discharges.

Using the VHF-GD technique it is also possible to achieve high deposition rates for $\mu\text{c-Si:H}$. In one approach, one can use of the so-called metastable-quenching effect of argon in SiH_4/H_2 plasmas; thus, an additional dissociation channel can be opened and the deposition rate hereby increased up to 10 \AA/s [42]. More recent experiments were based on an earlier study by Matsuda et al. [43] who had pointed out the beneficial role of enhanced plasma power for $\mu\text{c-Si:H}$ formation. Using this approach, deposition rates upto 16 \AA/s could be achieved at plasma excitation frequencies of 130 MHz [28,44]. The underlying mechanisms are as follows:

Using a high concentration of silane in hydrogen for the deposition leads, on one hand, to amorphous silicon growth, on the other hand, more radicals are also available for the rapid growth. At sufficiently high plasma power, a phase transition from a-Si:H to $\mu\text{c-Si:H}$ occurs (Fig. 5a). Hereby, high-quality $\mu\text{c-Si:H}$ could be obtained at high deposition rates [18,28,44]. Figure 5b shows the ratio of the OES (optical emission spectroscopy) lines of SiH^* (412 nm) and of atomic hydrogen at (656 nm) as a function of the dilution level and of the VHF power [28,45]. It can clearly be seen, that the effect of both dilution and of VHF power on the a-Si:H/ $\mu\text{c-Si:H}$ transitions can basically be monitored by the SiH^* to H_α ratio. Apart from high deposition rates, the VHF-GD process has, in contrast to the above-mentioned deposition techniques, the advantage of being applicable also to larger substrate sizes of up to $30 \times 40 \text{ cm}$ [46]. The implementation of uniform deposition of thin-film silicon by VHF-GD, onto even larger areas with higher plasma excitation frequencies is an important R&D issue.

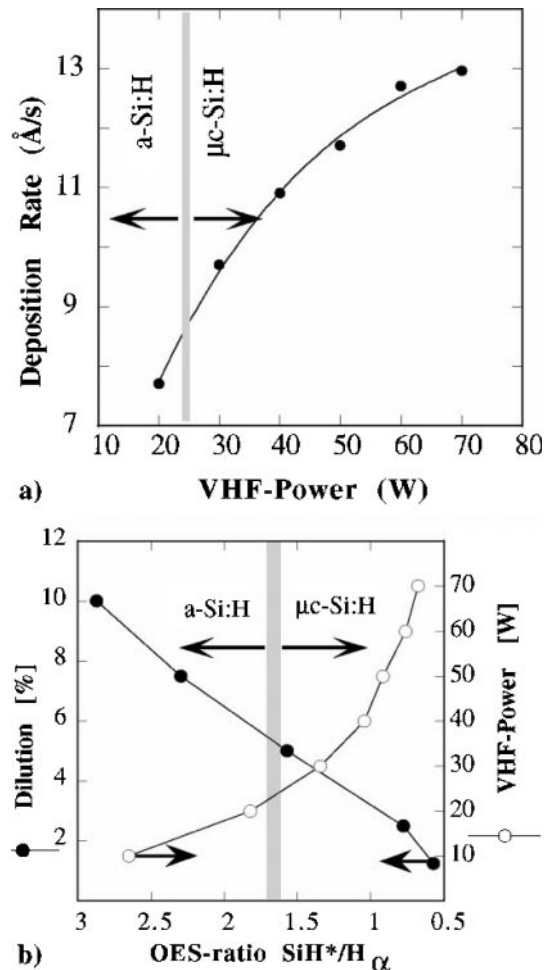


Fig. 5. a Deposition rate of $\mu\text{c-Si:H}$ as a function of the applied VHF power at 7.5% dilution ratio of silane into hydrogen plus silane [18]. b Correlation between the dilution ratio, the VHF power, and the OES emission-line ratio with the phase transition from a-Si:H to $\mu\text{c-Si:H}$ [45]. The dilution ratio is fixed at 7.5% (ratio of silane into hydrogen plus silane)

2 Microcrystalline-silicon-based solar cells

2.1 General statements

In Sect. 1.1 it was pointed out that the midgap character of the $\mu\text{c-Si:H}$ absorber material constitutes a necessary condition for obtaining “solar-grade” material. The link between the detected residual oxygen impurity level in the intrinsic layer and the spectral response of entirely $\mu\text{c-Si:H}$ *p-i-n* solar cells is shown in Fig. 6. High oxygen concentrations give rise to a loss in the electric field sustaining carrier drift and by that to an enhanced bulk recombination which can be observed as an accentuated decrease of the spectral response at long wavelengths. The techniques proposed in Sect. 1.1 for obtaining midgap material (compensation and purifying) could both be successfully applied to improve the red-light photocurrent collection [14–17].

Note that thanks to the smaller bandgap of $\mu\text{c-Si:H}$ when compared to a-Si:H and due to the enhancement of its “apparent” absorption when compared to monocrystalline-silicon (c-Si)-based cells, $\mu\text{c-Si:H}$ solar cells can generate, even at a thickness of 3.5 \mu m , photocurrent densities of around

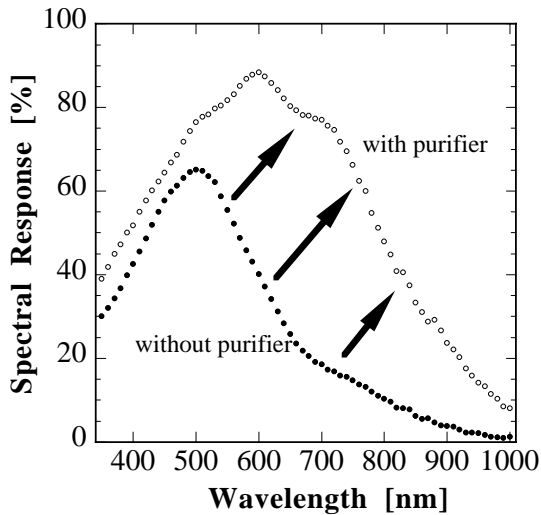


Fig. 6. Comparison of the spectral response (at zero bias voltage) of two entirely $\mu\text{c-Si:H}$ cells: one produced with a feedgas purifier and one without a purifier. The thickness of both cells is $2.8\ \mu\text{m}$ [15, 17]

Table 1. Best values of the parameters of single-junction $\mu\text{c-Si:H}$ solar cells obtained so far by IMT Neuchâtel [20, 21]

Quantity	Cell 1	Cell 2	Cell 3	Cell 4	Cell 5	Cell 6	Cell 7
$\eta/\%$	7.7	8.3	7.7	8.1	8.5	3.2	4.4
$J_{\text{SC}}/\text{mA}/\text{cm}^2$	25.3	25.2	21.5	23.2	22.9	18.4	17.9
$FF/\%$	67.9	68.2	71.1	68	69.8	30.5	41.8
V_{OC}/mV	448	483	503	512	531	568	592

$26\ \text{mA}/\text{cm}^2$, and this without fully optimized light-trapping. The best results so far obtained at our at our laboratory with entirely $\mu\text{c-Si:H}$ -based solar cells are summarized in Table 1 [20, 21].

The J_{SC} data of Table 1 are consistent with the absorption measurements of the material (see Fig. 2). Regarding the open-circuit voltage, one has at present no clear experimental evidence for what exactly causes either the high values of close to 600 mV or the low values of 450 mV. The interface passivation techniques that have been carried out, did not allow us to develop so far a consistent model about the V_{OC} -limiting mechanisms in $\mu\text{c-Si:H}$ solar cells. Nevertheless, as Table 1 points out, V_{OC} values as high as 592 are basically possible. On the other hand, the best fill factor values of about 70% so far obtained (at lower V_{OC} values) are quite satisfactory. However, the different experiments that have been carried out until now, could not furnish as yet a sample with all solar cell parameters being optimized simultaneously.

2.2 Stability

2.2.1 Light-soaking. Entirely microcrystalline-silicon solar cells are stable under light-soaking conditions [14, 17]. Figure 7 displays the experimental conditions and the results obtained for $\mu\text{c-Si:H}$ solar cells, in comparison with those for an amorphous silicon solar cell. Whereas the latter one degrades under sodium light of 6-sun intensity by about 50%, the $\mu\text{c-Si:H}$ cell remains completely stable even under 10 suns. This

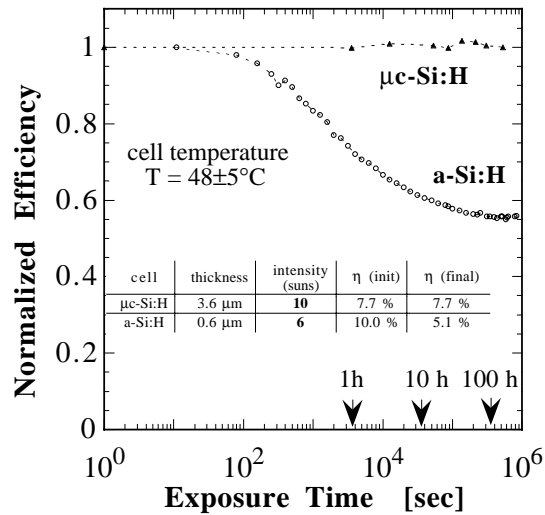


Fig. 7. Comparison of the normalized efficiency of an amorphous and a microcrystalline silicon cell, which were light-soaked under extreme conditions [14, 17]

is one of the most important aspects of $\mu\text{c-Si:H}$ cells and $\mu\text{c-Si:H}$ -based cells; it has also its implications for the micromorph cells described below.

2.2.2 Chemical stability. Individual $\mu\text{c-Si:H}$ thin films may show as a function of the deposition conditions a pronounced post-oxidation [47, 48] that gives rise to an increase in the lateral dark conductivity. However, such an effect could never be observed in entire solar cells [19]. It can be assumed that the doped layers in the solar cell configuration protect the intrinsic layer of the cell from such post-oxidation. Note, that even after more than one year of air exposure of $\mu\text{c-Si:H}$ cells no reduction in cell performance was observed.

3 “Micromorph” solar cells

3.1 General aspects

The combination of an amorphous silicon top cell with a microcrystalline silicon bottom cell to form a stacked tandem cell, is called the micromorph cell. In Fig. 8 a SEM cross section of a micromorph cell is shown.

The two different gap energies involved in the micromorph tandem cell of the top and of the bottom cell make a striking difference to the well-known double-junction a-Si:H/a-Si:H tandem cell. The concept of superposing two a-Si:H cells is based on the reduction in the Staebler–Wronski effect that can be obtained by keeping each individual i -layer as thin as possible and not on a better utilization of the solar spectrum.

In Fig. 9 a comparison of the spectral response curves and in Fig. 10 of the $I - V$ characteristics of both types of tandem cells is represented.

Whereas the double-junction concept for a-Si:H cells is useful for reducing light-induced degradation, one clearly sees in Fig. 9 that the micromorph tandem cells offer further the possibility of better utilization of the sun spectrum – a possibility that is also realized with a-Si:H/a-SiGe:H stacked cells, yet to a larger extent, as it is so far not possible

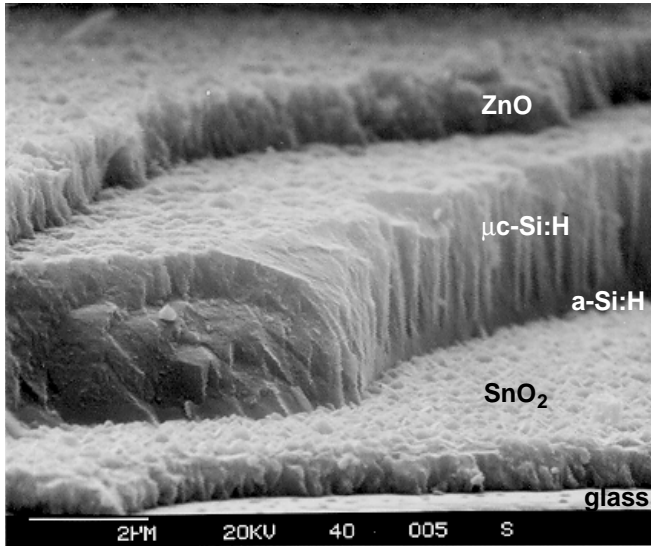


Fig. 8. Scanning electron micrograph (SEM) of the cross section of a micromorph tandem cell deposited on SnO₂-coated glass

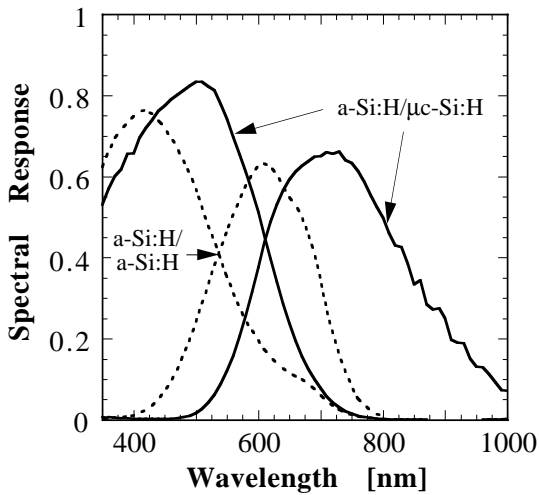


Fig. 9. Comparison of the spectral response of a double-stacked a-Si:H tandem cell and of a micromorph tandem cell. Note that the red spectral response of the micromorph cell is strongly extended towards long wavelengths [16]

to obtain low enough band gaps with device-quality amorphous silicon-germanium alloys.

3.2 Stability and state of the art of the cell performance

The stable $\mu\text{c-Si:H}$ bottom cell contributes to a better stability of the entire micromorph tandem cell under light-soaking. It could, in fact, be shown that the light-induced degradation of the micromorph cell is due to the amorphous top cell alone [17]. In a first attempt to a further increase in stable efficiency, one can use a thicker bottom cell that could deliver an enhanced photocurrent without running itself into stability problems. However, due to the required current matching, the thickness of the top cell must be increased as well, which leads again to stability problems. Note that despite the fact that the concept of a micromorph solar cell brings progress

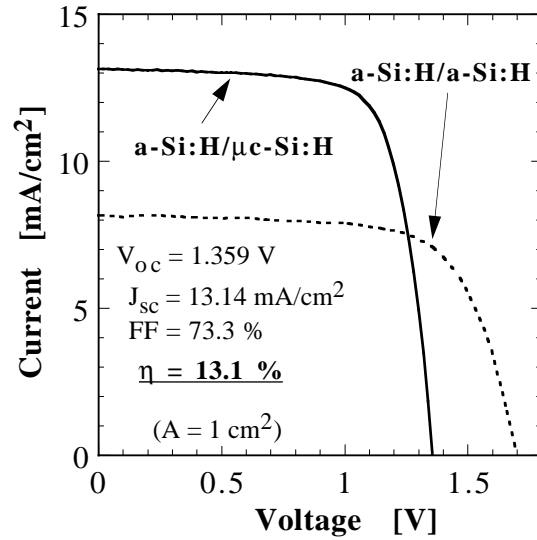


Fig. 10. Comparison of the $I-V$ characteristics of a double-stacked a-Si:H tandem cells and of a micromorph tandem cell [16]

via a new stable bottom cell into the thin-film silicon scenario, the stability of the amorphous silicon top cell remains still the crucial topic.

For enhanced stability of the a-Si:H cell many approaches have been investigated in the past. The most promising of them are the use of hydrogen dilution [49–51] and the hot wire deposition technique [52, 53]. As an example for the use of such approaches, Table 2 compares two micromorph tandem cells with incorporating hydrogen diluted and undiluted a-Si:H top cells after 1000 h of light-soaking.

The relative stability of the first type of top cells (H₂ dilution) is generally improved, but the reduced absorption (higher band gap) of such hydrogen-diluted a-Si:H layers limits the photocurrent of the top cell, and by that the current and the stable efficiency of the entire micromorph tandem cell. The relative stability of the second type of top cell is generally worse, but the enhanced absorption (lower band gap) increases the photocurrent of the entire tandem cell leading to better absolute stable micromorph cell efficiency.

Table 2 summarizes the best results that were obtained under outdoor conditions and compares them with measurements performed at an independent calibration laboratory (ISE-FhG).

Table 2. Parameters of stabilized micromorph tandem cells (1000 h light-soaked) measured at the ISE-FhG and under outdoor illumination of 93–95 mW/cm² (clear sky conditions in Neuchâtel at the 9th and 21st of July 1997). The given J_{SC} values are normalized to 100 mW/cm² for comparison

Quantity	Tandem cell A ^{a)}		Tandem cell B ^{b)}
	ISE-FhG Freiburg	outdoor at 25 °C	outdoor at 25 °C
$J_{SC}/\text{mA}/\text{cm}^2$	11.9	12.6	13.5
V_{OC}/V	1.34	1.343	1.284
FF	66.7	66.9	69.2
$\eta/\%$	10.7 ± 0.7	11.3 ± 0.6	12.0 ± 0.6

^{a)} H₂-diluted a-Si:H top, 0.21 μm

^{b)} undiluted a-Si:H top, 0.32 μm

3.3 Temperature coefficients of micromorph solar cells

For the assessment of new solar-cell concepts a further key question is: how many kWh per installed W_p can be obtained by corresponding solar modules throughout the lifetime of the solar cell (the lifetime can be assumed to be 20 years for most solar cell concepts). Because most solar modules have in practice to operate at relatively high temperatures, the temperature coefficient is, beside the cell and module efficiencies, a key parameter. The temperature coefficients of c-Si (wafer-based) cells, CIGD [54], and a-Si:H cells are documented.

Investigating the temperature coefficient of μ c-Si:H and micromorph cells one finds, that the temperature coefficient of the V_{OC} and J_{SC} values are quite similar to those found in c-Si cells, whereas the temperature coefficients of the fill factor (FF) are clearly reduced for micromorph and microcrystalline cells, in particular for those μ c-Si:H cells that have a high V_{OC} value (> 500 mV), as documented in [20]. In Figs. 11a,b the temperature behavior of the different solar cell parameters are normalized to the values measured at 25 °C.

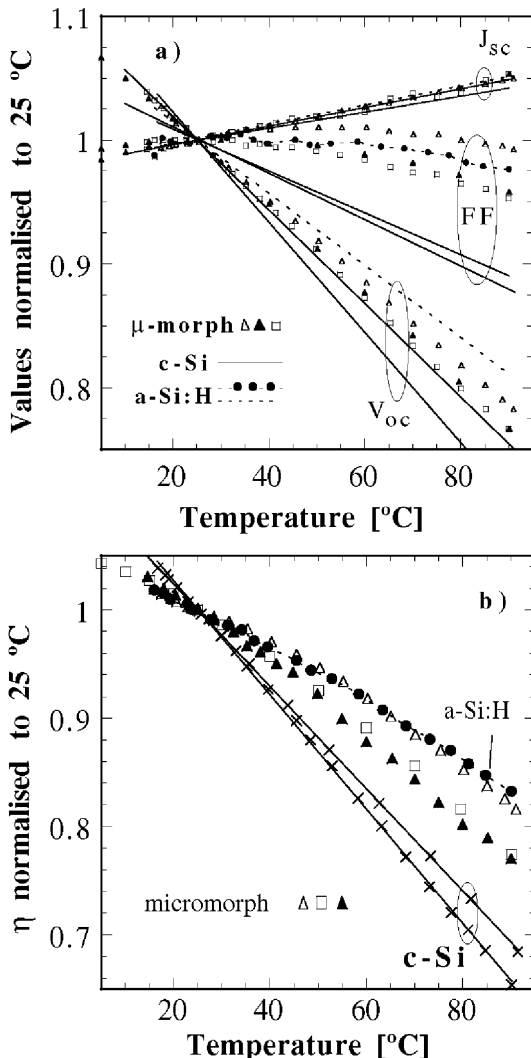


Fig. 11a,b. Temperature coefficient normalized to 25 °C of the parameters of micromorph tandem cells in function of cell temperature in comparison with those of crystalline and amorphous silicon: a) J_{SC} , FF , and V_{OC} ; b) Efficiency

Based on Fig. 11b one can conclude that the temperature coefficient of the micromorph cell efficiency lies between that of c-Si and that of a-Si:H cells. The relatively low value of this temperature coefficient make micromorph cells a favorable candidate for example for building integration of PV thin-film solar cells, especially in those cases where no special aeration of the facade can be provided to keep the temperature of the cell relatively low.

4 Problems to overcome and outlook

As discussed above, micromorph silicon solar cells are “real” tandem cells consisting of two absorber materials with two different gap energies. For all tandem solar cells the so-called photocurrent matching between top and bottom cell is imperative, in order to get the maximum power out of the cell. For micromorph cells, however, the difference in gap energies between top and bottom cells is pronounced, namely about 1 eV for the μ c-Si:H bottom cell and about 1.7 eV for the a-Si:H top cell. Thus, the current-matching problem appears here under a different angle.

Due to the difference in gap energies, the power generation in a micromorph cell is by nature shifted to the amorphous top cell because of the different open-circuit voltages of the individual cells. Note, the power from the top cell is larger by the ratio $V_{OC}(\text{top})/V_{OC}(\text{bottom})$ (900 mV/500 mV) than the power of the bottom cell. This is not an ideal situation because the top cell suffers from the Staebler–Wronski effect, whereas the stable bottom cell shares only one third of the total generated power. In order to achieve further improvements of micromorph solar cells, the following concepts or combinations of them must be realized:

1. The V_{OC} value of the bottom cell must be made as high as possible (such optimization, however, is “black art”).
2. An intermediate optical mirror between top and bottom cell can be implemented (see Fig. 12): this leads to enhanced light-trapping for the top cell [55, 56]. The top cell

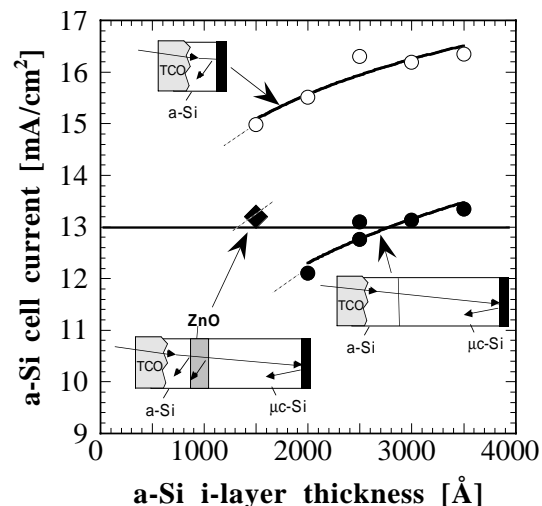


Fig. 12. Proof of concept for the implementation of an intermediate TCO mirror between the top and the bottom cell of a micromorph tandem cell. Note that the current of the a-Si:H top cell can thereby be clearly increased [55, 56]

is thereby kept thinner (leading to a reduced SWE), but it can still absorb enough light, thanks to an optical mirror.

3. Basically more stable amorphous silicon top cells should be obtained – this is as yet an unsolved problem in spite of intensive research effort.
4. Amorphous/microcrystalline silicon (a-Si:H/ μ c-Si:H/ μ c-Si:H) triple-junction cells can be implemented; hereby, the current-matching requirements over three individual cells shift the power generation towards the stable microcrystalline cells. Such triple-junction cells with a stable efficiency of 12% have been recently demonstrated [57].

The second point constitutes a promising new concept; first results can be seen.

All the above four points are the objective of further research work, and they contain in our opinion still a large space for improvement in stable efficiency. Figure 13 makes for example some predictions on efficiencies of micromorph cells if only the V_{OC} of the bottom cell is varied. The other solar cell parameters that have been assumed for Fig. 13, are the following: $V_{OC}(\text{top}) = 900$ mV, total fill factor $FF = 73\%$ and a total J_{SC} of 26 mA/cm^2 .

Figure 13 also summarizes the present state of microcrystalline/amorphous silicon tandem cell research activity, including both VHF-GD-deposited cells as well as plasma deposition methods carried out at higher temperatures (up to 550°C) [19, 22, 57, 58].

Apart from the conversion efficiency of the solar cells, obtaining a high deposition rate is another key issue. This issue will decide whether the micromorph solar cell might come into a region where its manufacturing becomes cost-competitive in terms of the production throughput or not; this question has to be clarified in the early stage of laboratory work.

Light-trapping is a further important issue for any thin-film solar concept because it helps to keep the total absorption of the cell but at reduced absorber thickness. Light-trapping

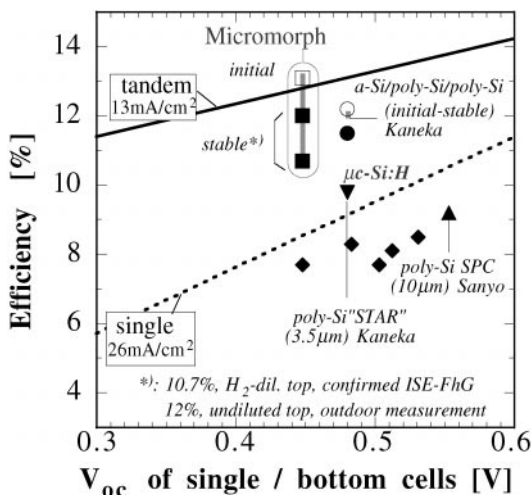


Fig. 13. Projected efficiencies of single-junction μ c-Si:H and micromorph tandem cells as a function of the V_{OC} of the μ c-Si:H bottom cells, assuming a total current of 26 mA/cm^2 , a fill factor of 73% and a V_{OC} of 900 mV for the a-Si:H cells (lines). Symbols represent experimentally obtained results [21]

allows furthermore to reduce the deposition time required and it improves the ratio between collection length and cell thickness. All these features are at present far from being optimized for the entire micromorph tandem cell and require further intensified research.

Beside the “classical” micromorph tandem structure there are yet other multiple-junction solar cell concepts that become interesting to implement with the help of microcrystalline silicon. One concept is the triple-junction combination a-Si:H/a-Ge:H/ μ c-Si:H. Another one is multiple junctions connected electrically in parallel rather than in series, as suggested by Green [59]. These concepts open further new possibilities for stimulating research.

5 Conclusions

Microcrystalline silicon is not just an individual new absorber material for solar cells, it contains a large morphological variety as described by the so-called Thornton diagram [60,61]. If one looks at the morphology of microcrystalline silicon the concept of an ideal isotropic semiconductor must be abandoned. Nevertheless, by varying the growth conditions, stable efficiencies of 10% can be achieved at deposition temperatures around 550°C [22] and of 8.5% at 200°C [20,21]. It transpires that the parameter field for optimization of microcrystalline silicon, as a function of its deposition conditions (i.e. as a function of its position in the Thornton diagram) contains not only one set of parameters, but a large span of parameters. It is a function of deposition temperature, pressure, gas flows, the presence and nature of the plasma used for deposition. Photovoltaic research is at the moment just starting to exploit thin-film crystalline silicon as an absorber material. Micromorph solar cells improve the stable efficiency of amorphous solar cells due to a better utilization of the solar spectrum; stable efficiencies of about 12% could be achieved with further potential for improvement. Nevertheless, laboratory research has always also to be aware of industrial requirements, and here the efficiency is only one of the issues. All deposition methods of thin-film solar cell concepts have to fulfill demands for large-area manufacturing at low production costs. There is indeed hope that the thin-film micromorph solar cell concept described in this paper can constitute a link between high-efficiency silicon solar cells in form of wafers (that are too expensive) and the potentially low-cost amorphous silicon technology with presently low efficiencies. One can argue [62] that the micromorph concept has the potential to become the concept for the next generation of thin-film solar cells, in view of its potential for high efficiency and low cost. One may also mention in this context the requirements of high reliability and of reduction in process energy and material flow.

Acknowledgements. This work was supported by the Swiss Federal Department of Energy BFE/OFEN No. 19431.

References

1. M.A. Green: In Proc. 2nd World Conf. Photovolt. Energy Conv. (Vienna 1998) pp. 1187–1192
2. R. Schäffler, E. Lotterer, R. Menner, B. Dimmler: In Proc. 14th Europ. Photovolt. Solar Energy Conf. (Barcelona, Spain 1997) p. 1266
3. H.W. Schock, A. Shah: In Proc. 14th Europ. Photovolt. Solar Energy Conf. (Barcelona, Spain 1997) p. 2000
4. D. Bonnet, M. Harr: In Proc. 2nd World Conf. Photovolt. Energy Conv. (Vienna 1998) pp. 397–402
5. J. Yang, A. Banerjee, K. Lord, S. Guha: In Proc. 2nd World Conf. Photovolt. Energy Conv. (Vienna 1998) pp. 387–390
6. D.E. Carlson, R.R. Arya, L.F. Chen, R. Oswald, J. Newton, K. Rajan, R. Romero, F. Willing, L. Yang: In Proc. NREL/SNL Photovoltaics Program Review, AIP Conference **394** (AIP, Woodbury, New York 1997) p. 479
7. W. Frammelsberger, P. Lechner, H. Rübél, H. Schade: In Proc. 14th Europ. Photovolt. Solar Energy Conf. (Barcelona, Spain 1997) p. 2006
8. R. Bergmann, R. Brendel, M. Wolf, P. Lölgen, J.H. Werner: In Proc. 25th IEEE Photovolt. Energy Conf. (Washington 1996) p. 365
9. A.L. Fahrenbruch, R.H. Bube: In *Fundamentals of Solar Cells* (Academic Press, New York, London 1983) p. 352
10. S. Veprek, V. Marecek: Solid State Electron. **11**, 683 (1968)
11. S. Veprek, M.G. J. Veprek-Heijman: Plasma Chem. Plasma Processing **11**, 323 (1991)
12. S. Veprek, M. Heintze, F.-A. Sarott, M. Jurcik-Rajman, P. Willmott: Mater. Res. Soc. Symp. Proc. **118**, 3 (1988)
13. H. Curtins, N. Wyrsh, A. Shah: Electron. Lett. **23**, 228 (1987)
14. J. Meier, R. Flückiger, H. Keppner, A. Shah: Appl. Phys. Lett. **65**, 860 (1994)
15. P. Torres, J. Meier, R. Flückiger, U. Kroll, J.A.A. Selvan, H. Keppner, A. Shah, S.D. Littlewood, I.E. Kelly, P. Giannoulès: Appl. Phys. Lett. **69**, 1373 (1996)
16. J. Meier, S. Dubail, R. Flückiger, D. Fischer, H. Keppner, A. Shah: In Proc. 1st World Conf. Photovolt. Energy Conf. (Hawaii 1994) p. 409
17. J. Meier, P. Torres, R. Platz, S. Dubail, U. Kroll, J.A.A. Selvan, N.P. Vaucher, C. Hof, D. Fischer, H. Keppner, A. Shah, K.-D. Ufert, P. Giannoulès, J. Koehler: Mater. Res. Soc. Symp. Proc. **420**, 3 (1996)
18. P. Torres, J. Meier, U. Kroll, N. Beck, H. Keppner, A. Shah: In Proc. 26th IEEE Photovolt. Energy Conf. (Anaheim 1997) p. 711
19. J. Meier, S. Dubail, J. Cuperus, U. Kroll, R. Platz, P. Torres, J.A. Anna Selvan, P. Pernet, N. Beck, N. Pellaton Vaucher, C. Hof, D. Fischer H. Keppner, A. Shah: J. Non-Cryst. Solids **227-230**, 1250 (1998)
20. J. Meier, H. Keppner, S. Dubail, U. Kroll, P. Torres, P. Pernet, Y. Ziegler, J.A. Anna Selvan, J. Cuperus, D. Fischer, A. Shah: Mater. Res. Soc. Symp. Vol. 507 (San Francisco 1998) pp. 139–144
21. J. Meier, H. Keppner, S. Dubail, Y. Ziegler, L. Feitknecht, P. Torres, Ch. Hof, U. Kroll, D. Fischer, J. Cuperus, J.A. Anna Selvan, A. Shah: 2nd World Conf. Photovolt. Energy Conv. (Vienna 1998), in print
22. K. Yamamoto, M. Yoshimi, T. Suzuki, Y. Tawada, Y. Okamoto, A. Nakajima: 2nd World Conf. Photovolt. Energy Conv. (Vienna 1998) pp. 1284–1289
23. A.R. Middy, J. Guillet, J. Perrin, J.E. Bouree: Mater. Res. Soc. Symp. Proc. **420**, 289 (1996)
24. J. Cifre, J. Bertomeu, J. Puigdollers, M.C. Polo, J. Andreu, A. Lloret: Appl. Phys. A **59**, 645 (1994)
25. J.K. Rath, A. Barbon, R.E.I. Schropp: J. Non-Cryst. Solids **227**, 1277 (1998)
26. A.A. Howling, J.-L. Dorier, C. Hollenstein, U. Kroll, F. Finger: J. Vac. Sci. Technol. A **10**, 1080 (1992)
27. M. Heintze, R. Zedlitz: Prog. Photovoltaics: Res. Appl. **1**, 213 (1993)
28. P. Torres: Ph.D. Thesis, University of Neuchâtel
29. P. Torres, R. Flückiger, J. Meier, U. Kroll, V. Shklover, A. Shah: In Proc. 13th Europ. Photovolt. Solar Energy Conf. (Nice, France 1995) p. 1638
30. K. Keppner, U. Kroll, P. Torres, J. Meier, D. Fischer, M. Goetz, R. Tscharnner, A. Shah: Proc. 25th IEEE Photovolt. Energy Conf. (Washington 1996) p. 669
31. U. Kroll, J. Meier, H. Keppner, S.D. Littlewood, I.E. Kelly, P. Giannoulès, A. Shah: Mater. Res. Soc. Symp. Proc. **377**, 39 (1995)
32. U. Kroll, J. Meier, H. Keppner, A. Shah, S.D. Littlewood, I.E. Kelly, P. Giannoulès: J. Vac. Sci. Technol. A **13**, 2724 (1995)
33. G. Vergani, M. Succi, E.J. Thrush, J.A. Crawly, W. van der Stricht, P. Torres, U. Kroll: Proc. of the Institute of Environmental Sciences, 262 (1997)
34. S. Veprek, Z. Iqbal, R.O. Kühne, P. Capezzuto, F.-A. Sarott, J.K. Gimzewski: J. Phys. C: Solid State Phys. **16**, 6241 (1983)
35. G. Willeke: In *Amorphous & Microcrystalline Semiconductor Devices*, II, ed. by J. Kanicki (Artech House, Boston, London 1992) p. 55
36. F. Wang, H.N. Liu, Y.L. He, A. Schweiger, R. Schwarz: J. Non-Cryst. Solids **137-138**, 511 (1991)
37. C. Wang, G. Lucovsky: Proc. 21th IEEE Photovolt. Energy Conf., (1990) p. 1614; M.J. Williams, C. Wang, G. Lucovsky: J. Non-Cryst. Solids **137-138**, 737 (1991)
38. N. Beck, J. Meier, J. Fric, Z. Remes, A. Poruba, R. Flückiger, J. Pohl, A. Shah, M. Vanecek: J. Non-Cryst. Solids **198-200**, 903 (1996)
39. M. Vanecek, A. Poruba, Z. Remes, N. Beck, M. Nesladek: J. Non-Cryst. Solids **227-230**, 967 (1998)
40. A. Poruba, Z. Remes, J. Springer, M. Vanecek, A. Fejfar, J. Kocka, P. Torres, A. Shah: In Proc. 2nd World Conf. Photovolt. Energy Conv. (Vienna 1998) pp. 781–784
41. N. Imajyo: J. Non-Cryst. Solids **198-200**, 935 (1995)
42. H. Keppner, P. Torres, J. Meier, R. Platz, D. Fischer, U. Kroll, S. Dubail, J.A. Anna Selvan, N. Pellaton Vaucher, Y. Ziegler, R. Tscharnner, C. Hof, N. Beck, M. Goetz, P. Pernet, M. Goerlitzer, N. Wyrsh, J. Vuille, J. Cuperus, A. Shah, J. Pohl: Mater. Res. Soc. Symp. Proc. **452**, 865 (1997)
43. A. Matsuda: J. Non-Cryst. Solids **59-60**, 767 (1983)
44. P. Torres, H. Keppner, J. Meier, U. Kroll, N. Beck, A. Shah: Phys. Status Solidi /RRN-97-039, <http://www.vchgroup.de/akademie-verlag/>, Phys. Status Solidi A **163**, R9 (1997)
45. P. Torres, U. Kroll, H. Keppner, J. Meier, E. Sauvain, A. Shah: Proc. 5th European Conf. on Plasma Processes (St Petersburg 1998) p. 855
46. L. Sansonnens, A.A. Howling, Ch. Hollenstein: Mater. Res. Soc. Symp. Proc. (San Francisco 1998) p. 541
47. S. Veprek, Z. Iqbal, R.O. Kühne, P. Capezzuto, F.-A. Sarott, J.K. Gimzewski: J. Phys. C 6241 (1983)
48. M. Goerlitzer, P. Torres, N. Beck, N. Wyrsh, U. Kroll, H. Keppner, J. Pohl, A. Shah: J. Non-Cryst. Solids **227-230**, 996 (1998)
49. J. Yang, X. Xu, S. Guha: Mater. Res. Soc. Symp. Proc. **336**, 687 (1994)
50. R. Platz, D. Fischer, C. Hof, S. Dubail, J. Meier, U. Kroll, A. Shah: Mater. Res. Soc. Proc. **420**, 51 (1996)
51. R. Platz, D. Fischer, S. Dubail, A. Shah: Solar Energy Mater. Solar Cells **46**, 157 (1997)
52. A.H. Mahan, J. Carapella, B.P. Nelson, R.S. Crandall, I. Balberg: J. Appl. Phys. **69**, 6728 (1991)
53. Y. Ziegler, S. Dubail, C. Hof, U. Kroll, A. Shah: In Proc. 26th IEEE Photovolt. Energy Conf. (Anaheim 1997) p. 687
54. K. Bücher: In Proc. 13th Europ. Photovolt. Solar Energy Conf. (Nice, France 1995) p. 2097
55. D. Fischer, S. Dubail, J.A. Anna Selvan, N. Pellaton Vaucher, R. Platz, C. Hof, U. Kroll, J. Meier, P. Torres, H. Keppner, N. Wyrsh, M. Goetz, A. Shah, K.-D. Ufert: In Proc. 25th IEEE Photovolt. Energy Conf. (Washington 1996) p. 1053
56. N. Pellaton Vaucher, J.-L. Nagel, R. Platz, D. Fischer, A. Shah: In Proc. 2nd World Conf. Photovolt. Energy Conv. (Vienna 1998) pp. 728–731
57. K. Yamamoto, T. Suzuki, M. Yoshimi, A. Nakajima: In Proc. 14th Europ. Photovolt. Solar Energy Conf. (Barcelona, Spain 1997) p. 1018
58. T. Baba, T. Matsuyama, S. Tsuge, K. Wakisaka, S. Tsuda: Proc. 13 EPVSEC (1995) p. 1708
59. L.M. Koshier, S.R. Wenham, M.A. Green: Proc. 2nd World Conf. on Photovolt. Solar Energy Conv. (Vienna 1998) pp. 292–295
60. J.A. Thornton: J. Vac. Sci. Technol. A **11**, 666 (1974)
61. J.A. Thornton: Ann. Rev. Mater. Sci. **7**, 239 (1977)
62. K. Saito, M. Sano, K. Matuda, T. Kondo, T. Nishimoto, K. Ogawa, I. Kajita: In Proc. 2nd World Conf. Photovolt. Energy Conf. (Vienna 1998) pp. 351–354